

Independent Torque Distribution Strategies for Vehicle Stability Control

Indrasen Karogal and Beshah Ayalew
Clemson University

Copyright © 2009 SAE International

ABSTRACT

This paper proposes and compares torque distribution management strategies for vehicle stability control (VSC) of vehicles with independently driven wheels. For each strategy, the following feedback control variables are considered turn by turn: 1) yaw rate 2) lateral acceleration 3) both yaw rate and lateral acceleration. Computer simulation studies are conducted on the effects of road friction conditions, feedback controller gains, and a driver emulating speed controller. The simulation results indicated that all VSC torque management strategies are generally very effective in tracking the reference yaw rate and lateral acceleration of the vehicle on both dry and slippery surface conditions. Under the VSC strategies employed and the test conditions considered, the sideslip angle of the vehicle remained very small and always below the desired or target values.

This study forms an essential step in the design and selection of actuators (e.g., in-wheel motors) for vehicle dynamics control of vehicles with independently driven wheels. Applications include certain powertrain architectures for pure electric or series hybrid electric and hydraulic hybrid vehicles with independent all wheel drives.

INTRODUCTION

Vehicle stability control (VSC), also called electronic stability control (ESC) or vehicle dynamics control (VDC), is an active vehicle safety system intended to

reduce driver loss of control of the vehicle by correcting the onset of vehicle instability. A number of studies suggest that VSC has the potential to reduce crashes resulting from such loss of control (1-3). In particular, if all vehicles were to be fitted with VSC systems, nearly one-third of all fatal crashes could be prevented and rollover risk can be reduced by as much as 80% (3).

The control strategy behind current vehicle stability control systems generates the required corrective yaw moment in various ways and reduces the deviation of vehicle behavior from its normal behavior. Different types of vehicle stability control systems can be identified and categorized (4) as a) differential braking systems b) active steering systems and c) active torque distribution systems. Most vehicle stability control systems in the market today are brake-based. With these brake-based strategies the vehicle speed is compromised. By comparison, active torque distribution systems can maintain vehicle speed. Most of these are differential-based torque biasing or torque vectoring systems (5, 6). In this paper, we focus on a specific class of active torque distribution systems suitable for vehicles with fully independent wheel drives.

Energy and environmental considerations have led to the accelerated research and development of hybrid electric vehicles (HEVs), electric vehicles (EVs), fuel cell vehicles (FCVs), and hydraulic hybrid vehicles (HHVs). Electric or hydraulic propulsion systems employed in these vehicles can be configured with independent in-wheel or on-board drive motors (7, 8). That is, the electric or hydraulic motors of the powertrain in these vehicles

The Engineering Meetings Board has approved this paper for publication. It has successfully completed SAE's peer review process under the supervision of the session organizer. This process requires a minimum of three (3) reviews by industry experts.

All rights reserved. No part of this publication may be reproduced, stored in a retrieval system, or transmitted, in any form or by any means, electronic, mechanical, photocopying, recording, or otherwise, without the prior written permission of SAE.

ISSN 0148-7191

Positions and opinions advanced in this paper are those of the author(s) and not necessarily those of SAE. The author is solely responsible for the content of the paper.

SAE Customer Service: Tel: 877-606-7323 (inside USA and Canada)
Tel: 724-776-4970 (outside USA)
Fax: 724-776-0790
Email: CustomerService@sae.org

SAE Web Address: <http://www.sae.org>

Printed in USA



9-2009-01-0456

SAE International

can be integrated into each wheel or drive each wheel independently and can also be controlled independently (9, 10). The good controllability of electric or hydraulic motors (via the manipulation of their torque outputs) offers an opportunity to achieve vehicle stability control by modulating the independent drive torque at each wheel of the vehicle. This research is primarily concerned with the study of VSC architectures and strategies for such vehicles.

The rest of the paper is organized as follows. First, the mathematical model of the vehicle used for the development and analysis of the proposed stability control strategies is described. Second, the adopted feedback controllers and the proposed torque distribution strategies are discussed. Third, the effectiveness of proposed torque distribution strategies and feedback control techniques is evaluated and compared through computer simulations. Finally, the paper concludes with observations and inferences from the simulation results.

VEHICLE MODEL

The vehicle model adopted includes longitudinal, lateral and yaw motions as well as the rotational dynamics of the four wheels. It ignores the presence of the suspension and so excludes heave, pitch and roll of the vehicle. Figure 1 shows the schematic diagram for the vehicle model adopted. δ_f is the steering angle for the front wheels, which in this work is assumed to be identical for the left and right wheels during cornering.

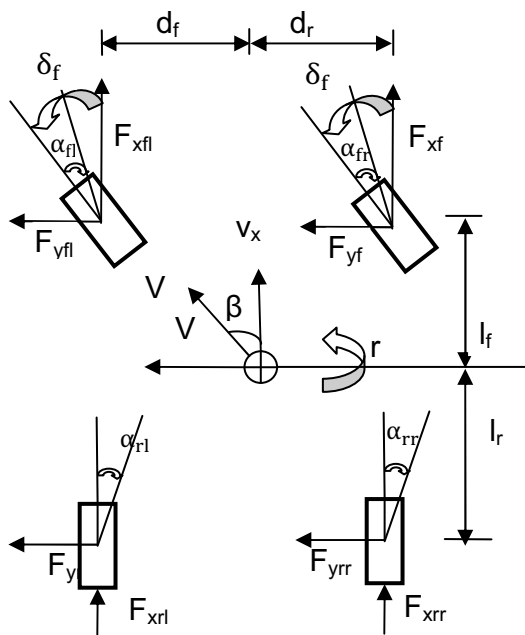


Figure 1 Schematic of vehicle model (11)

The longitudinal, lateral and yaw equations of motion for a rigid vehicle in planar motion are given, respectively, by:

$$m(\dot{v}_x - \dot{\psi}v_y) = \sum F_x = F_{xfl_b} + F_{xfr_b} + F_{xrl_b} + F_{xrr_b} - \frac{1}{2} C_D \rho A v_x^2 \quad (1)$$

$$m(\dot{v}_y + \dot{\psi}v_x) = \sum F_y = F_{yfl_b} + F_{yfr_b} + F_{yrl_b} + F_{yrr_b} \quad (2)$$

$$I_{zz} \ddot{\psi} = \sum M_Z = l_f (F_{yfl_b} + F_{yfr_b}) - l_r (F_{yrl_b} + F_{yrr_b}) + \frac{d_f}{2} (F_{xfr_b} - F_{xfl_b}) + \frac{d_r}{2} (F_{xrr_b} - F_{xrl_b}) + \sum_{i=1}^4 M_{Zi} \quad (3)$$

TIRE AND WHEEL MODEL

In this research, Pacejka (Magic Formula) formulations of tire models are used. The general form (12) is:

$$Y(x) = D \sin(C \tan^{-1}\{Bx - E(Bx - \tan^{-1}(Bx))\}) \quad (4)$$

where $Y(x)$ is either longitudinal force F_x with x as longitudinal slip ratio or lateral force F_y with x as the side slip angle or self-aligning moment M_z with x as the side slip angle. The coefficients in the above equation in each case depend on the tire design and the road and load conditions.

The normal force acting on, for example, the front left wheel due to longitudinal and lateral accelerations (a_x and a_y , respectively) of the vehicle, is given by:

$$F_{zfl} = \frac{mg l_r}{2l} - \frac{m a_x h}{2l} - m a_y \left(\frac{l_r}{l}\right) \left(\frac{h}{d_f}\right) \quad (5)$$

The relevant equation for the angular acceleration of the front left wheel is:

$$T_{fl} - R_{fl} F_{xfl_w} = J_{\omega fl} \dot{\omega}_{fl} \quad (6)$$

The linear velocity of the front left wheel center is:

$$v_{\omega fl} = \left(v_x - \psi \frac{d_f}{2}\right) \cos \delta_f + \left(v_y + \psi l_r\right) \sin \delta_f \quad (7)$$

The longitudinal slip ratio, S , for the front left wheel is:

$$S_{\omega ro} = \left(\frac{R_{fl} \omega_{fl}}{v_{\omega lo}} - 1\right) \quad (8)$$

The side slip angle, α , for each wheel can be obtained from the lateral and longitudinal components of the wheel center velocity with respect to the C.G. of the vehicle.

$$\alpha_{fl} = \delta_f - \tan^{-1} \left(\frac{v_y + \psi l_r}{v_x - \psi \frac{d_f}{2}} \right) \quad (9)$$

The above set of equations, repeated for all wheels, describes a non-linear model of the vehicle system. These equations were implemented in the graphical programming interface of MATLAB/ SIMULINK.

VEHICLE STABILITY CONTROL

The basic functionality of a vehicle stability control (VSC) system involves reducing the deviation of the vehicle behavior from its normal behavior and maintaining the vehicle slip angle within specified bounds. The VSC develops a corrective yaw moment based on the deviation between actual and desired vehicle responses and passes this information to lower level actuator controllers. These lower level actuator (electric or hydraulic motors, braking systems etc.) controllers manage the application and distribution of the required drive torque or braking effort to the wheels. In this simulation study, the non-linear vehicle model described above is considered to give the actual vehicle responses while the desired responses are obtained from a bicycle model of the vehicle. In most cases, the desired responses of the state variables are chosen from steady state responses of a standard reduced order (bicycle) model to road wheel steering angle input. For a given road wheel steering angle, δ , the following expressions give the desired yaw rate (r_d), lateral acceleration (a_{y_d}) and side slip angle (β_d), respectively (13) :

$$r_d = \frac{v_x * \delta}{1 + K_{us} * v_x^2} \quad (10)$$

$$a_{y_d} = \frac{v_x^2 * \delta}{1 + K_{us} * v_x^2} \quad (11)$$

$$\beta_d = \left(\frac{l_f * l_r * \left(\frac{1}{l_f} - \frac{m * v_x^2}{l_r * C_2} \right) * \delta}{l^2 - m * \left(\frac{l_f}{C_2} - \frac{l_r}{C_1} \right) * v_x^2} \right) \quad (12)$$

The lateral acceleration and yaw rate error are, respectively:

$$e_{a_y} = a_y - a_{y_d} \quad (13)$$

$$e_r = r - r_d \quad (14)$$

Where a_y and $r = \dot{\psi}$ are the actual values of the corresponding vehicle states (lateral acceleration and yaw rate, respectively) obtained from the non-linear vehicle model. The errors e_{a_y} and e_r are the feedback variables used in the VSC as will be detailed below.

The control architecture adopted is depicted in Figure 2.

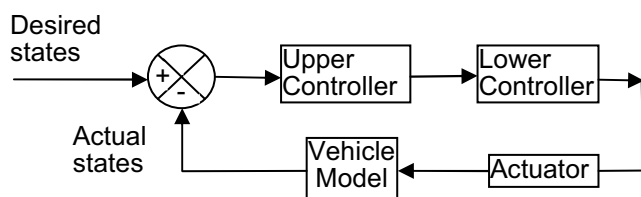


Figure 2 Schematic of VSC architecture.

Upper Controller: The objectives of the upper controller are to ensure yaw stability control by computing and

commanding a desired value of corrective yaw moment from the lower controller. Inputs to the upper controller are the errors between the desired and actual vehicle states. In this work, a PI controller is taken as the upper controller.

Lower Controller: The lower (level) controller ensures that the corrective yaw moment demanded by the upper controller is converted to a demanded action on a lower level physical vehicle parameter. This parameter, which is generally a braking, driving or steering effort, should be properly controlled to achieve the desired corrective yaw moment.

In this study, the dynamics of the actuators/motors themselves are neglected in the analysis. That is perfect actuation is assumed. The torque distribution management system manages the torque distribution between the wheels to achieve the desired yaw moment commanded by the upper level controller.

YAW MOMENT CONTROL THROUGH TORQUE TRANSFER

Front to Rear Torque Transfer: As more drive torque is transferred to the front, the longitudinal forces on the front wheels increase. In turn, the longitudinal slip ratio of the front axle grows while that of the rear axle drops. This also leads to a decrease in the lateral forces generated by the front tires compared to the rear ones as explained by the friction ellipse (4,14). Thus, increased torque transfer from the rear to the front wheels of the vehicle, induces an understeering effect.

Side to Side Torque Transfer: When the driving torque on inner wheel is increased in comparison to that of the outer wheel, the longitudinal forces on the inner wheels increase while those on the outer wheels decrease. Consequently, the lateral forces generated by the inner wheels decrease while those by the outer wheels increase. As can be explained by equation (3), the differences in longitudinal forces produce significant amount of negative (counter-to-turn) yaw moment while the differences in lateral forces a smaller positive yaw moments. Thus, a net yaw moment in a direction opposite to turn is generated, leading to understeer.

Based on the physical consequence of longitudinal force distribution as discussed above, two approaches of distributing torque to each wheel of the vehicle are identified: the 'torque-ratio' approach, proposed in (15) and the 'differential torque transfer' approach presented in this work.

The torque-ratio approach utilizes two PI controllers which control two torque ratios (side to side and front to rear) matched to two corresponding feedback variables. The front to rear torque ratio is controlled by using the yaw rate error, while the left to right torque ratio is controlled by using the lateral acceleration error. The simulation results presented in (15) for this 'torque-ratio'

approach are encouraging. The variation in torques is constrained by the two ratios and the total torque on the vehicle is kept constant. The approach simplifies the control problem by reducing the control variables from four (each of four individual wheel torques) to two (two torque ratios) and reduces the freedom of torque distribution by imposing the constraints on the total torque.

In this study, we focus on yaw moment generation through side to side torque transfer involving differential torque transfer i.e. addition or/and subtraction of corrective torques (the torque produced by upper controller of VSC system) to the individual wheel torques. This doesn't necessarily constrain the total torque to a constant value. This approach provides an additional degree of freedom in torque distribution thus allowing the modulation of independent torque to each wheel. In this study, this approach has been closely studied and implemented in simulations. The choice of appropriate feedback control variables (yaw rate and lateral acceleration) that go with this approach will also be detailed in the next sub-sections.

Base Torque and Speed Control

In practice, various standard test maneuvers are executed at constant or nearly constant speed. Considering this practice, speed control (driver emulation) is introduced in some of the simulated tests. A simple PI function is used for speed controller.

$$\Delta T_v = K_{p_v} e_v + K_{i_v} \int e_v dt \quad (15)$$

Where the error function e_v is defined as the difference between actual forward velocity v_x and the desired (set) forward velocity of the vehicle, v_{x_des} .

$$e_v = v_x - v_{x_des} \quad (16)$$

In general, in all simulations involving speed controlled (constant speed) maneuvers; the total torque ΔT_v is assumed to be equally distributed between all wheels. Accordingly, in case of speed controlled VSC, the distributed (speed control) torque is added to the corrective torques produced by VSC at each wheel. In case of no speed control, constant torques termed as 'base torques' are provided to each wheel and added to the corrective torques produced by the VSC strategy to each wheel. The total base torques on the left and right sides of the vehicle are given, respectively, by:

$$T_L = T_{fl} + T_{rl} \quad (17)$$

$$T_R = T_{fr} + T_{rr} \quad (18)$$

Where $T_{fl}, T_{rl}, T_{fr}, T_{rr}$ are the individual base torques acting on the individual wheels. Note that the speed controller is tuned independent of the VSC controllers discussed below.

Yaw Rate Control

The difference between actual yaw rate and the desired yaw rate is an obvious measure of deviation of the vehicle from its desired course and hence can be used to create the corrective yaw moment using an appropriate controller. In this work, the required differential torque, ΔT_r , is evaluated from a PI type function of yaw rate error, e_r and is given by:

$$\Delta T_r = K_{p1} e_r + K_{i1} \int e_r dt \quad (19)$$

Where the e_r is the yaw rate error.

Figure 3 shows the vehicle in different scenarios, including left or right hand turning and exhibiting possible understeering or oversteering behaviors. The figure also includes the sign conventions adopted in this work. Starting from these scenarios, the following torque distribution strategies are conceived to achieve the desired corrective yaw moment. The strategies apply the torques to the *left and right* wheels of the vehicle, *irrespective of the direction of turn*.

Strategy 1: Addition of corrective VSC torques only to left wheels. In this strategy, the corrective torques are added only to left wheels while no corrective torques are applied to the right wheels. That is:

$$T_{L_new} = T_L + \Delta T_r \quad (20)$$

$$T_{R_new} = T_R \quad (21)$$

Strategy 2: Subtraction of corrective VSC torques only from right wheels. The corrective torques are applied only to right wheels. That is:

$$T_{L_new} = T_L \quad (22)$$

$$T_{R_new} = T_R - \Delta T_r \quad (23)$$

For both of the above two strategies, the VSC differential corrective torque is:

$$\Delta T_r > 0 \quad (\text{Oversteering condition}) \quad (24)$$

$$\Delta T_r < 0 \quad (\text{Understeering condition}) \quad (25)$$

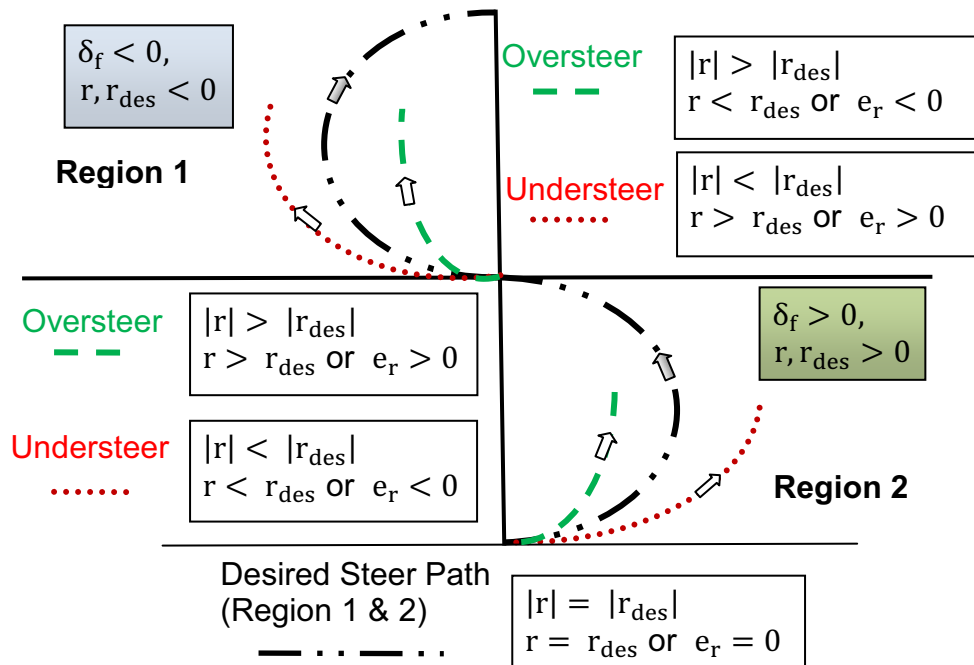


Figure 3 Schematic of vehicle in various scenarios and adopted sign conventions

Strategy 3: Switching corrective torque addition between left and right wheels. VSC torques are applied to the left or right part of the vehicle depending on the sign of the yaw rate error, e_r . For a positive yaw rate error (oversteering condition for left hand turn or understeering condition for right hand turn), the drive torques on the left wheels are increased while for a negative yaw rate error (understeering condition for left hand turn or oversteering condition for right hand turn), the drive torques on the right wheels are increased. Mathematically, these are described as follows:

$$\text{When } e_r > 0, T_{L_new} = T_L + |\Delta T_r| \quad (26)$$

$$\text{When } e_r < 0, T_{R_new} = T_R + |\Delta T_r| \quad (27)$$

Strategy 4: Corrective VSC torques: add to left wheels and subtract from the right wheels. In this strategy, half the corrective VSC torques are added to the left wheels and half of them are subtracted from the right wheels. This will not alter the total torque on the vehicle. That is:

$$T_{L_new} = T_L + \frac{\Delta T_r}{2} \quad (28)$$

$$T_{R_new} = T_R - \frac{\Delta T_r}{2} \quad (29)$$

Lateral Acceleration Control

With the lateral acceleration as the feedback variable, the required differential torque, ΔT_{ay} , can be evaluated from the PI type function in a similar way as was done above for yaw rate control. This torque is given by:

$$\Delta T_{ay} = K_{p2}e_{ay} + K_{i2} \int e_{ay} dt \quad (30)$$

Where, e_{ay} is the lateral acceleration error.

The four strategies for torque distribution can be similarly applied for lateral acceleration control as was done for yaw rate control. For example, a typical strategy (Strategy 4) can be expressed mathematically as:

$$T_{L_new} = T_L + \frac{\Delta T_{ay}}{2} \quad (31)$$

$$T_{R_new} = T_R - \frac{\Delta T_{ay}}{2} \quad (32)$$

Combined Yaw Rate and Lateral Acceleration Control

This considers both the yaw rate and lateral acceleration errors in computing the VSC corrective torque. In so doing, this approach attempts to indirectly consider body side slip angle deviations. Again, this can be used with any of the four strategies discussed above. However, for brevity, Strategy 4) has been chosen to analyze this combined feedback control. The final wheel torques are given by:

$$T_{lf_new} = T_{lf} + \frac{\Delta T_r}{2} + \frac{\Delta T_{ay}}{2} \quad (33)$$

$$T_{lr_new} = T_{lr} + \frac{\Delta T_r}{2} + \frac{\Delta T_{ay}}{2} \quad (34)$$

$$T_{rf_new} = T_{rf} - \frac{\Delta T_r}{2} - \frac{\Delta T_{ay}}{2} \quad (35)$$

$$T_{rr_new} = T_{rr} - \frac{\Delta T_r}{2} - \frac{\Delta T_{ay}}{2} \quad (36)$$

Figure 4 summarizes the various combinations of feedback control and torque distribution strategies considered in this paper.

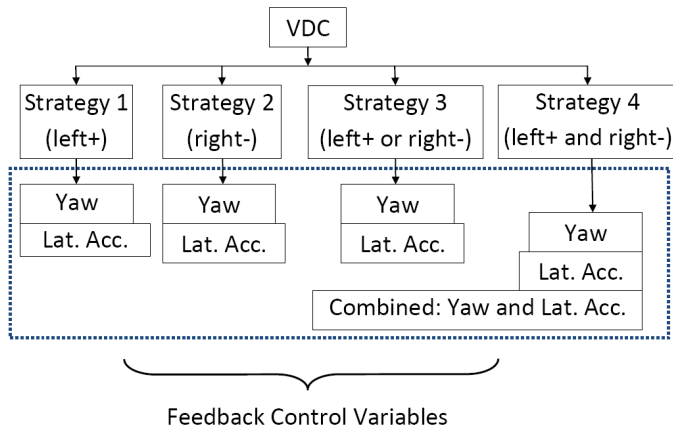


Figure 4 Torque distribution strategies and feedback control techniques

RESULTS AND DISCUSSIONS

For the simulations conducted in this work, the vehicle and tire data correspond to that for a large front wheel drive saloon car, available in Appendix A of (13). In order to analyze the effectiveness of the proposed VSC strategies, some standard test maneuvers were considered and appropriately modified: The first test involves road wheel angle steering input in the form of "Sine with Dwell" with a sine wave at 0.7 Hz frequency and a 400 ms delay beginning at the second peak amplitude" (see Figure 5). This test has been modified from FMVSS 126 ESC Test (16) to use road wheel steer angle inputs consistent with our model. The other test is a standard J-turn with the step applied at 1 sec and achieving the required road-wheel angle (RWA) of 3 degrees in 0.1 sec (ramping with the slope of 30 deg/s).

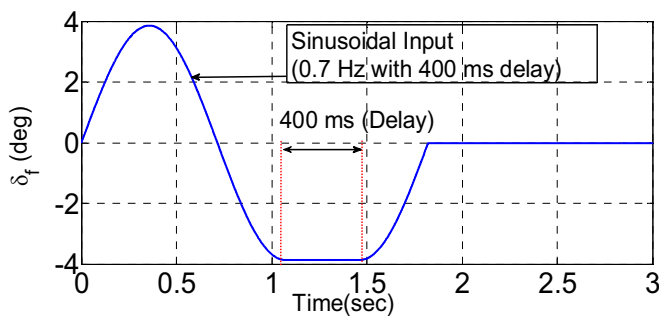


Figure 5 Sine with dwell test steer input

YAW RATE CONTROL

The corrective differential torque computed from yaw rate feedback according to Eq (19) is considered first. The effects of speed control (driver emulation for test), road friction conditions (different coefficients of friction between road and tires, μ), feedback controller gains and the choice of the torque distribution strategies are investigated.

Effect of VSC and Speed Control

The vehicle performance parameters, yaw rate and lateral acceleration are compared for the vehicle with and without VSC (labeled VDC in all plots) in the presence or absence of speed controller (driver maintaining vehicle speed at 80 kmph). Torque distribution Strategy 4 is implemented on the vehicle with VSC on dry asphalt road conditions ($\mu = 1$).

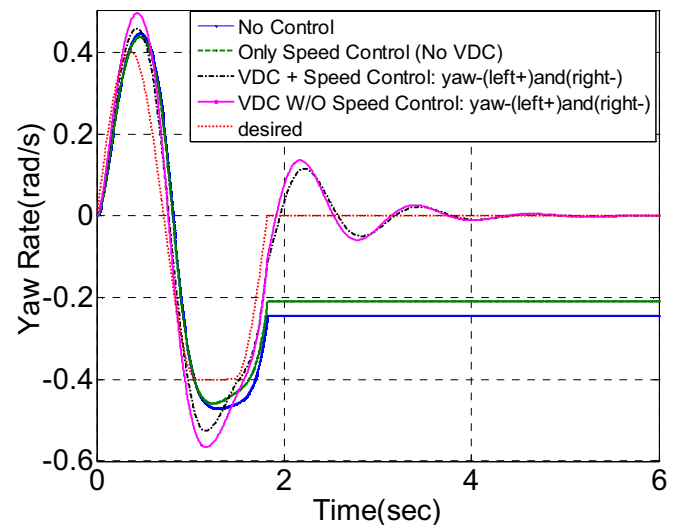


Figure 6 Yaw rate responses (with and without VSC), Strategy 4, Dry asphalt surface ($\mu = 1$)

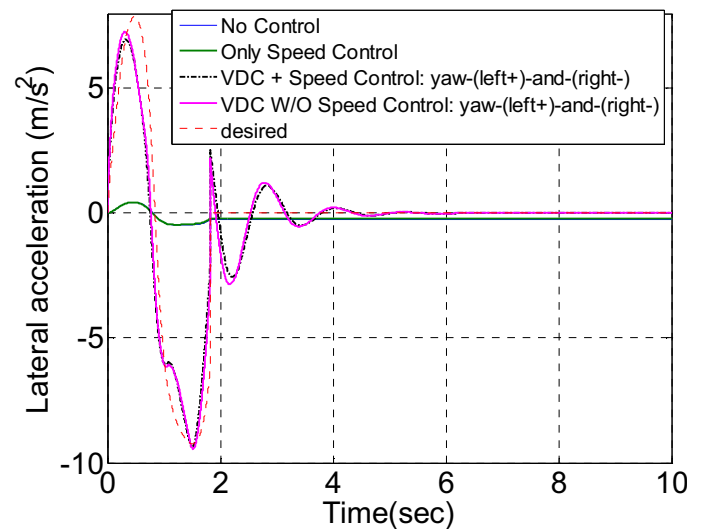


Figure 7 Lateral acceleration response (with and without VSC), Strategy 4, Dry asphalt surface ($\mu = 1$)

The time history plot of the yaw rate response (Figure 6) clearly shows that VSC (VDC) with and without speed control is able to return to zero steer motion (straight-line motion) and maintain it while the uncontrolled system is not. The VSC system tracks the desired yaw rate closely. Similarly, Figure 7 shows that the VSC system tracks the desired lateral acceleration while the uncontrolled system fails to do so.

To study the tracking ability for sudden changes in steering angle, we consider a step steer input (J-turn) of 3 deg RWA at a speed of 80 kmph on dry asphalt road, and with VSC Strategy 4. Figure 9 shows the results.

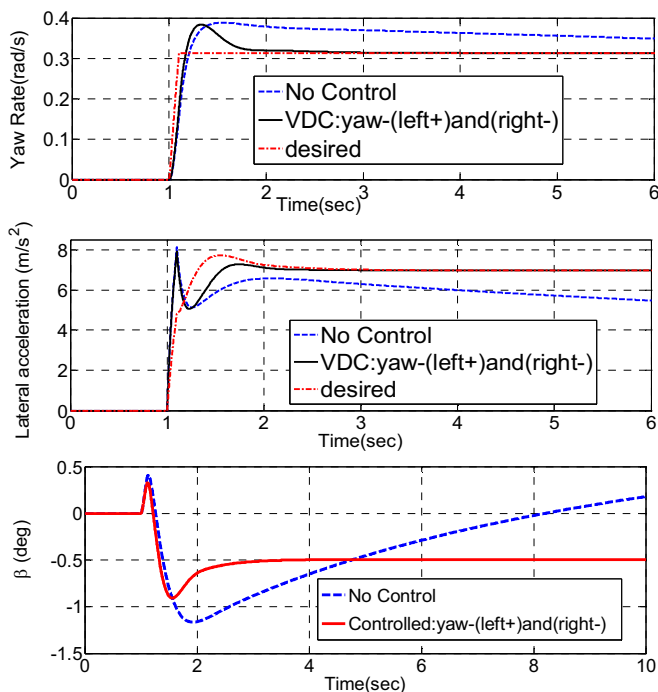


Figure 8 Simulation results of vehicle response to J-turn input (with speed control): Strategy 4, $\mu = 1$

All three responses show an overshoot in response to the step steer for the selected set of controller gains. The oscillations settle down quickly and good tracking ability is observed for yaw rate and lateral acceleration responses with the VSC strategy 4. The sideslip angle also remains very small.

Effect of Controller Gains on Performance:

Three sets of PI controller gains were used for comparative study of the effect of controller gains on VSC performance. Figure 9 shows the yaw rate response and the resulting motor torques at the front left wheel of the vehicle. We observe the improvement in the tracking ability and the faster return to the straight-line motion with increasing controller gains. Table 1 gives the values of the controller gains used and a summary of the effect of controller gains on performance.

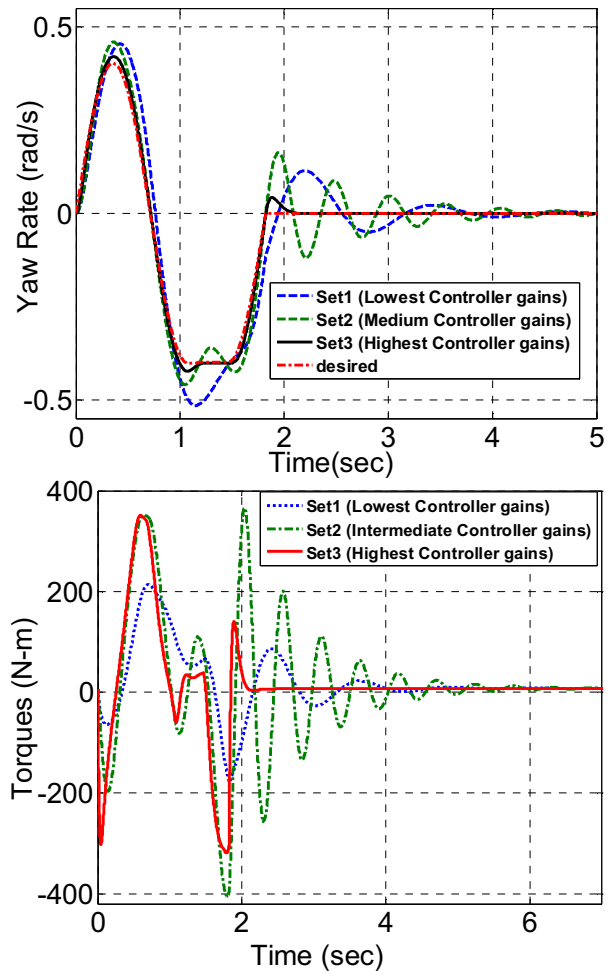


Figure 9 Effect of controller gains on yaw rate response and motor torque on front left wheel

Table 1 Vehicle performance for different controller gains (Controller: yaw rate error feedback)

	Set 1 (lowest gains) $K_P = 1000,$ $K_I = 1000,$	Set 2 (medium gains) $K_P = 1000,$ $K_I = 10000$	Set 3 (highest gains) $K_P = 1000,$ $K_I = 100000$
Yaw rate tracking ability (deviation error e_{tr} in rad^2/s^2)	17.0551	11.4607	0.7107
Oscillations at the start of straight-line motion			
Maximum overshoot	0.115	0.165	0.042
Settling time	2.7	2.7	0.3
Controller effort (Torques on front left wheels) (Max. and Min. Torque in Nm)	214,-180	352,-400	352,-320

Comparison of Torque Distribution Strategies

To compare the different torque distribution strategies, simulations were carried out with and without speed control. Set 1 of controller gains (the lowest set in Table 1) giving the slowest responses was taken to more clearly depict the differences between the results.

a. Comparisons of VSCs with Speed Control (80 kmph)

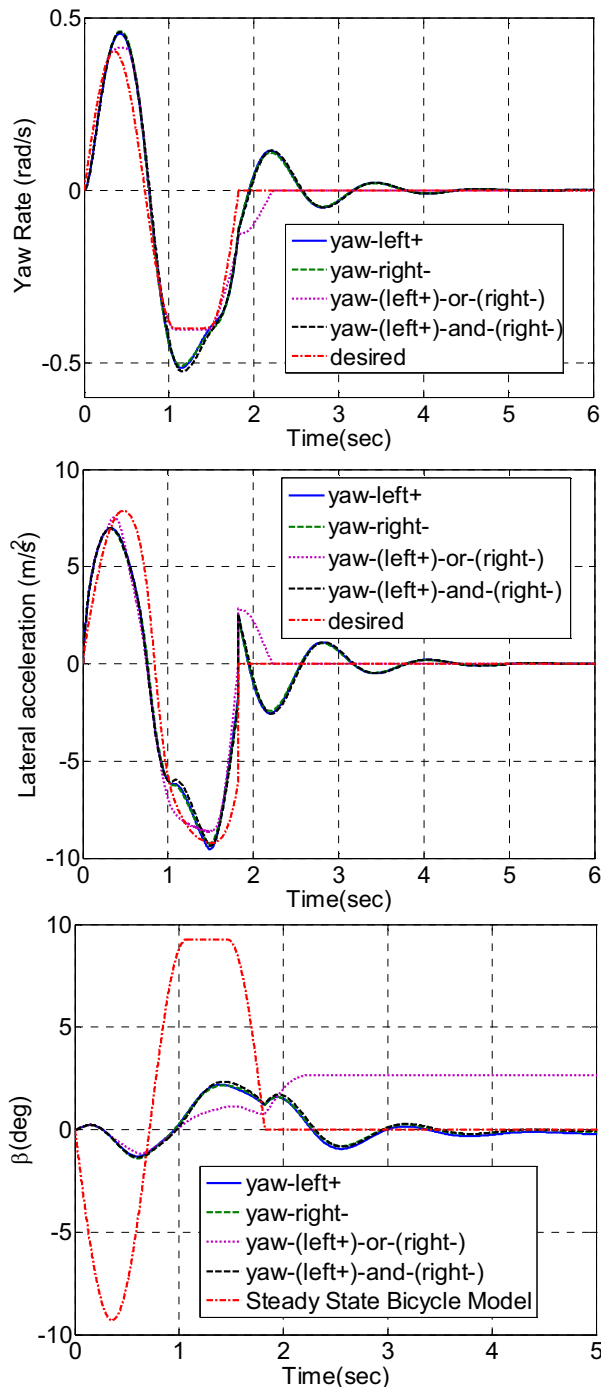


Figure 10 Comparison of VSC torque distribution strategies: vehicle responses (Yaw rate feedback with speed control, dry asphalt surface ($\mu = 1$))

As observed from the yaw rate and lateral acceleration responses in Figure 10, Strategies 1, 2 and 4 show quite similar time history plots while strategy 3 gives much better results in terms of tracking ability and oscillating behavior. Strategy 3 shows higher overshoot at the end of maneuver but settles down quickly. The vehicle returns to its straight-line motion very fast without any oscillations. The yaw rate feedback control, in these test cases, also kept the side slip angle small (even less than the steady state values obtained from the reference bicycle model).

Although Strategy 3 appears to give better tracking ability, it shows high fluctuations in wheel torques (not shown in here) as it involves a discontinuous switching function. Further analysis and approximation of the switch may be required to improve this strategy and achieve realistic steady wheel torques.

In order to compare the control effort required by Strategies 1, 2 and 4, input torques to individual wheels are plotted as shown in Figure 11. It can be seen that the maximum torque required is highest for Strategy 2 amongst all, while Strategy 1 requires a lower maximum torque and the lowest straight-ahead torque.

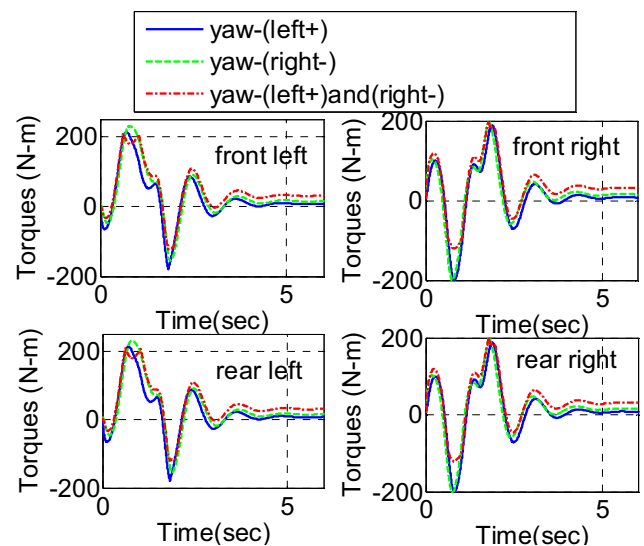


Figure 11 Comparison of VSC torque distribution strategies: Torque on individual wheels (Yaw rate feedback with speed control, dry asphalt ($\mu = 1$))

It should be recalled that the corrective VSC torques are added only to the left wheels for Strategy 1 while they are subtracted only from the right wheels in case of Strategy 2. But as observed from Figure 11, the time history plots of the final torques corresponding to both of these strategies are close and overlapping during most of the time. This can be explained as follows. The torques developed by the speed controller are such that when the yaw rate controller corresponding to Strategy 1 adds positive torques to the left wheels of the vehicle, the overall torque on the vehicle increases and hence the vehicle speed. The speed controller develops

negative torques and adds equally to the corrective yaw torques on all the wheels, thus the net torques on outer wheels are negative while those on inner wheels are positive but of accordingly reduced magnitudes. The variations in the torques on individual wheels corresponding to Strategy 2 can be explained similarly.

Table 2 Summary of quantitative comparison of VSC torque distribution strategies (Controller: Yaw rate feedback, with speed control)

Parameters	Strategy .1	Strategy .2	Strategy .3	Strategy .4
Yaw rate tracking ability (deviation error, e_{tr} in rad^2/s^2)	17.055	17.011	10.532	18.61
Lateral acceleration tracking ability (deviation error, e_{tay} in $m2/s4$)	10016	9392	10714	1022.1
Oscillations at the start of straight-line motion				
Max overshoot	0.1145	0.109	Nil	0.115
Approx. Settling time (sec)	@ 3	@ 3	@0.5	@ 3
Controller effort (Max.Torque, Min.Torque in Nm)	213, -180	230, -154	240, -150	210, -120

b. Comparisons of VSCs without Speed Control

This case (the speed controller switched OFF) is analyzed to make the distinction between the torque distribution strategies clearer. The yaw rate response for this case is shown in Figure 12.

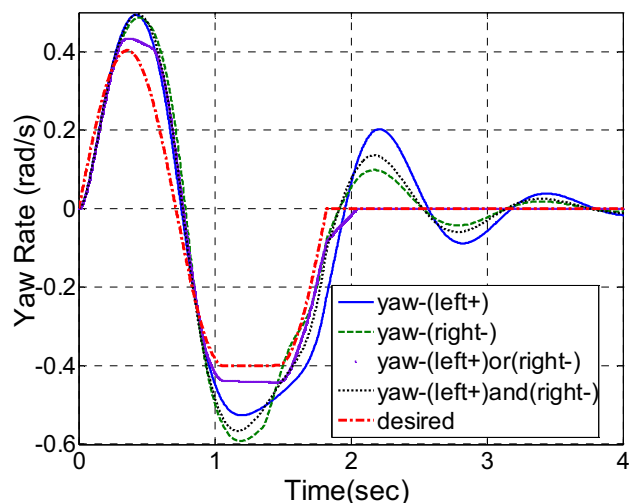


Figure 12 Comparison of VSC torque distribution strategies: Yaw rate response (Yaw rate error feedback without speed control, dry asphalt surface ($\mu = 1$))

Strategy 3 gives much better results compared to Strategies 2 & 4 while Strategy 1 is the worst in terms of yaw rate tracking ability. However, Strategy 3 has the difficulties associated with the discontinuous switching function as mentioned above. The resultant final wheel torques corresponding to each of Strategies 1 and 2, on one set of wheels (right wheels in case of Strategy 1 or left wheels in case of Strategy 2) are constant as shown in Figure 13.

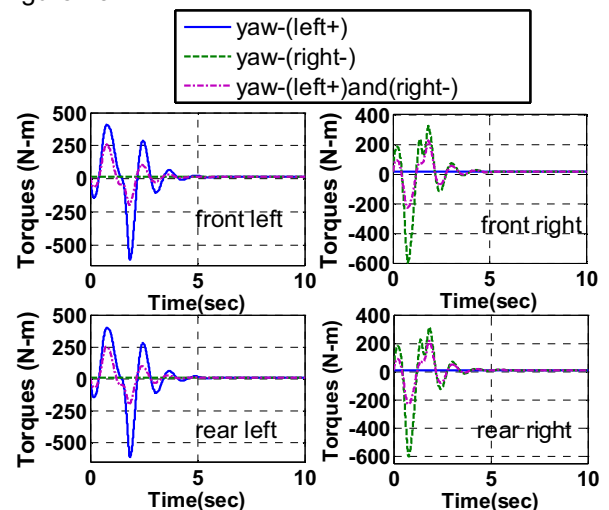


Figure 13 Comparison of VSC torque distribution strategies: Torque on individual wheels (Yaw rate feedback without speed control, dry surface ($\mu = 1$))

For both cases (with and without speed control), strategy 4 is the best based on the comparison of the performance parameters listed in Table 2 above.

LATERAL ACCELERATION CONTROL

Lateral acceleration control was implemented on a slippery surface (low-coefficient of friction, $\mu = 0.3$) with and without speed control, to evaluate VSC effectiveness under more severe conditions. Figure 14 shows a typical result for torque distribution Strategy 4 with speed control while using lateral acceleration feedback. It shows that it tracks the desired responses very closely throughout the maneuver, and maintains small sideslip angles.

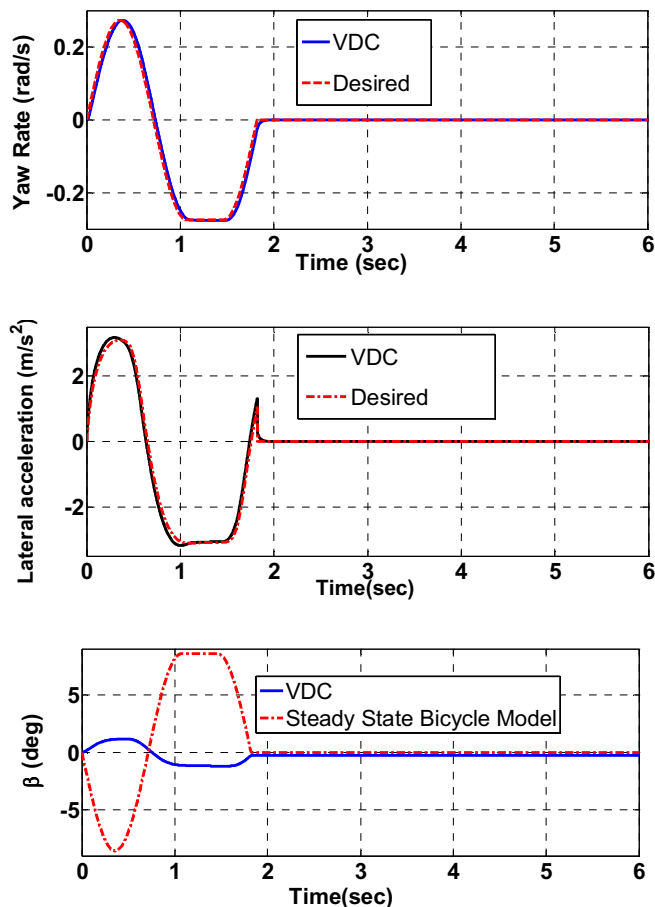


Figure 14 Vehicle responses under VSC Strategy 4 with lateral acceleration feedback with speed Control (40 kmph) on slippery surface ($\mu = 0.3$)).

COMPARISONS OF YAW RATE CONTROL, LATERAL ACCELERATION CONTROL, AND COMBINED (YAW + LATERAL ACCELERATION) CONTROL

To compare the three feedback controllers' use in VSC, simulations were carried out on a slippery surface ($\mu = 0.3$) for simulating sever conditions, using VSC torque distribution Strategy 4. The nominal initial vehicle speed is set at 50kmph, but is not controlled. This combination is chosen for brevity of presentation. The results are given in Figure 15.

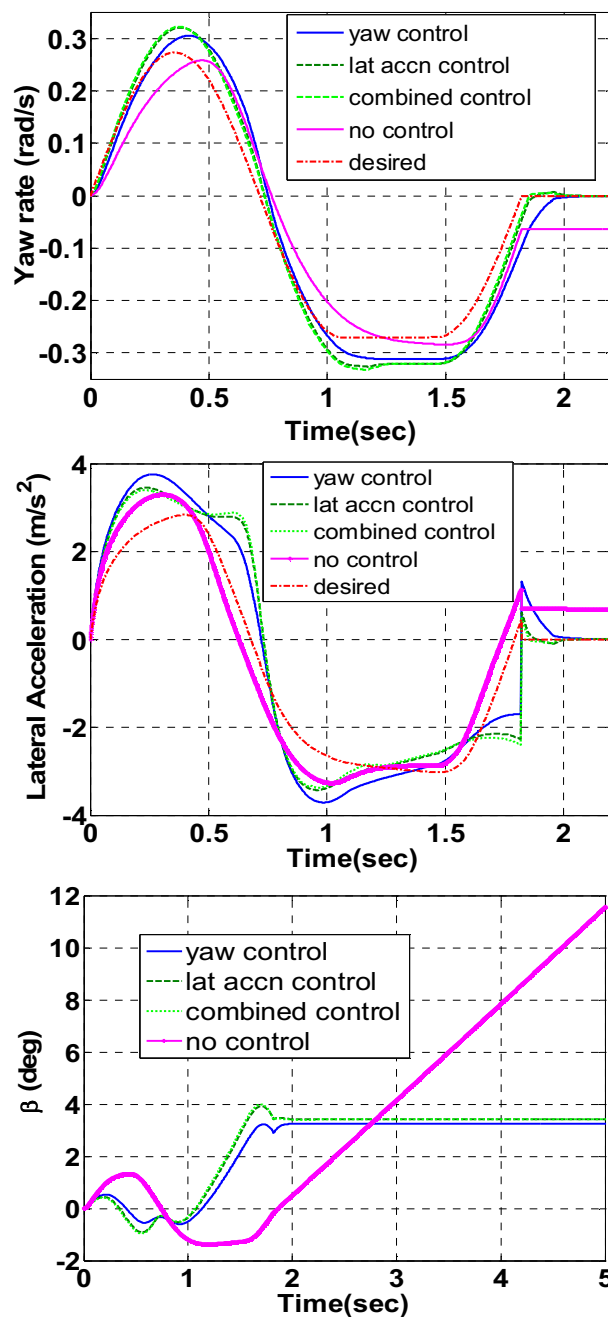


Figure 15 Comparison of feedback controllers: Vehicle responses. Slippery surface ($\mu = 0.3$), without speed control

As can be seen in Figure 15, the yaw rate and lateral acceleration time history plots for the simulation test conditions do not show any significant differences between the three feedback controllers. The sideslip angle of the uncontrolled vehicle starts deviating at the end of the maneuver and the vehicle fails to maintain the desired course (slip angle) while any of the VSC feedback controllers limit the sideways drift.

The comparison of the torque profiles in Figure 16 shows that the combined (yaw + lateral acceleration)

control produces higher peaks due to high gains chosen for each of the PI loops considered.

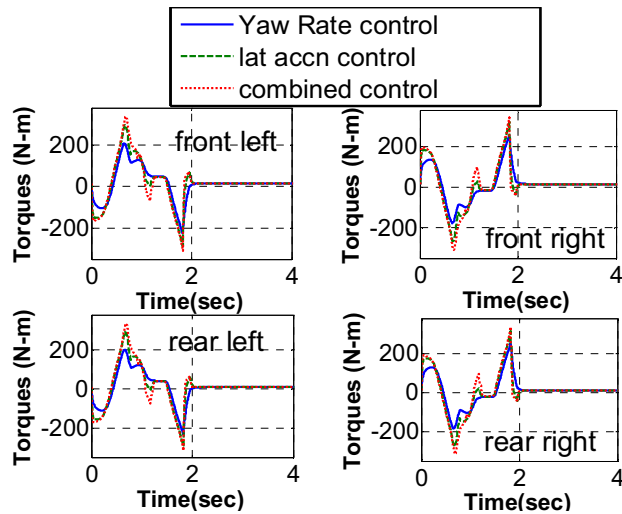


Figure 16 Comparison of feedback controllers: Torque on individual wheels. Slippery surface ($\mu = 0.3$), without speed control

CONCLUSION

In this paper, four torque distribution strategies were proposed for possible stability control of vehicles with independent wheel drive systems. The four torque distribution strategies, which are based on a differential torque transfer approach, attempt to achieve yaw moment control through the feedback control variables: yaw rate and lateral acceleration and a combination of yaw rate and lateral acceleration.

Through simulations all three feedback controllers were found to be effective in tracking the desired yaw rate and lateral acceleration of the vehicle on dry and slippery surface conditions. Sideslip angle of the vehicle also remained very small and always below the desired values. For the simulated test conditions and test vehicle considered, this rendered separate side slip angle control unnecessary. The Strategy 4 (VSC corrective torques being added to left wheels and subtracted from right wheels) was found to be the best one amongst all torque distribution strategies considering various control parameters and its ability to achieve realistic results.

The study presented in this paper constitutes first steps towards the selection of a combination of torque-distribution strategy, components and feedback controllers for active stability control of vehicles with independent wheel drives. For example, the computed torque magnitudes and time responses can be factored into the design or selection of the electric motors or hydraulic motors for independent drive systems. The performance of the system can be evaluated in further detail by introducing more degrees of freedom in the vehicle model, using more robust/non-linear yaw

moment controllers and incorporating effective wheel slip control.

NOMENCLATURE

F_x	longitudinal tire force
F_y	lateral tire force
F_z	lateral tire force
α	tire slip angle
β	vehicle sideslip angle
M_z	Total yaw moment acting on the vehicle about the z-axis
v_x	longitudinal velocity in vehicle plane [m/s]
v_y	lateral velocity in vehicle plane
a_x	longitudinal acceleration in vehicle plane
a_y	lateral acceleration in vehicle plane
δ_f	front wheel steering angle
T	torque acting on wheel
ω	angular speed of wheel
S	longitudinal slip ratio
I_{zz}	total vehicle moment of inertia about the z-axis
r (or $\dot{\Psi}$)	vehicle yaw rate
m	total mass of the vehicle
l_f	distance of front axle from C.G. of vehicle
l_r	distance of rear axle from C.G. of vehicle
l	wheel base
h	height of C.G. of the vehicle above ground
d_f	front wheel track
d_r	rear wheel track
R	wheel radius
M_{zi}	self aligning torque of i^{th} wheel ($i = 1, 2, 3, 4$)
g	acceleration due to gravity
C_1, C_2	Cornering stiffness of front and rear tires (averaged per axle) respectively
K_{us}	understeer gradient of the vehicle
K_p, K_i, K_d	proportional, integral and derivative gains of the PID controller respectively
ΔT	differential corrective torque to be transferred
e_{ay}, e_r	errors corresponding to lateral acceleration and yaw rate control respectively.

SUBSCRIPTS

fl	front left wheel
fr	front right wheel
rl	rear left wheel
rr	rear right wheel
L	left part of vehicle (includes front and rear left tires)
R	right part of vehicle (includes front and rear right tires)
a_y	lateral acceleration control applied
r	yaw rate control applied

REFERENCES

1. M., Aga and A., Okada, Analysis of Vehicle Stability Control(VSC)'s Effectiveness from Accident Dataproceedings of the 19th international conference on the enhanced safety of vehicles, 2003.

2. E.Green, Paul and Woodrooffe, John, (2006). The estimated reduction in the odds of loss-of-control type crashes for sport utility vehicles equipped with electronic stability control
3. IIHS. INSURANCE INSTITUTE FOR HIGHWAY SAFETY News Release.
http://www.iihs.org/news/2006/iihs_news_061306.pdf.
[Online] June 13, 2006.
4. Rajamani, Rajesh. Vehicle Dynamics and Control. Springer, 2005. pp. 221-256.
5. Jonathan C. Wheals, Hanna Baker, Keith Ramsey and Will Turner, Torque Vectoring AWD Driveline: Design, Simulation, Capabilities and Control, SAE, 2004-01-0863, 2004.
6. Kroppe, John Park and William J., Dana Torque Vectoring Differential Dynamic Trak™, SAE, 2004-01-2053, 2004.
7. B.Jacosen,(2002). Potential of electric wheel motors as new chassis actuators for vehicle maneuvering. Journal of Automobile Engineering, Proceedings of the Institution of Mechanical Engineers Part D, Vol. 216, pp. 631-640.
8. A.J.Achten, Peter, The Hybrid Transmission, SAE International, 07CV-64, 2007.
9. R.Sims and B.bates, Electric Vehicle :Driving Toward Commercialization, SAE, 1997.
10. E.Esmailzadeh, G.R.Vossoughi and A.Goodarzi, (2001), Dynamic Modeling and analysis of a four motorized wheels electric vehicle, International Journal of Vehicle Mechanics and Mobility no.3,, Vol. 35, pp. 163-194.
11. Shuibo Zheng, Houjun Tang,Zhengzhi Han,Yong Zhang (2006). Controller Design for vehicle stability enhancement, Control Engineering Practice 14, 1413-1421, Shanghai.
12. Pacejka, Hans. B. Tyre and vehicle dynamics. Second Edition,Oxford: Butterworth Heinemann, 2002. pp. 172-197.
13. A.Ghoneim, Youssef, et al. (2000), Integrated chassis control system to enhance vehicle stability. , International Journal of Vehicle Design, Vol. 23, pp. 124-144.
14. Genta, G. Motor Vehicle Dynamics, Modeling and Simulation, Series on Advances in Mathematics for Applied Sciences. Vol. 43, 1997.
15. P.Osborn, Russell and Shim, Taehyun, Independent Control of All-Wheel-Drive Torque Distribution, SAE Automotive Dynamics,Stability & Controls Conference. 2004-01-2052, 2004.
16. Federal Motor Vehicle Safety Standards;Electronic Stability Control Systems; Controls and Displays. Department Of Transportation, National Highway Traffic Safety Administration (NHTSA), DOT. Final Rule. Docket No. NHTSA-200727662, RIN: 2127AJ77, 2007.